Biochemical Journal Immediate Publication. Published on 29 Jan 2007 as manuscript BJ20061182

Title Page

Distinct roles of the C_2A and the C_2B domain of the vesicular Ca^{2+} sensor synaptotagmin 9 in endocrine β-cells

Florence Grise[*], Nada Taib[+], Carole Monterrat[*], Valérie Lagrée [*] and Jochen Lang[*]

Université de Bordeaux 1, Jeune Equipe 2390[*] et UMR 5144 CNRS Mobios[+], Institut Européen de Chimie et Biologie, 2 Av. Robert Escarpit, F-33607 Pessac, France

Address correspondence to:
J. Lang, Tel. +33 540 00 3349; Fax +33 540 00 3348; e-mail j.lang@iecb.u-bordeaux.fr

Running title: Roles of synaptotagmin 9 C_2A and C_2B domain

Key Words: Ca^{2+}, translocation, membranes, secretory granules, exocytosis

Biochemical Journal Immediate Publication. Published on 29 Jan 2007 as manuscript BJ20061182

Synopsis

Synaptotagmins form a family of calcium-sensor proteins implicated in exocytosis and these vesicular transmembrane proteins are endowed with two cytosolic calcium-binding C_2 domains, C_2A and C_2B. Whereas the isoforms syt1 and 2 have been studied in detail, less is known on syt9, the calcium sensor of endocrine secretion such as insulin release from large dense core vesicles in pancreatic β-cells. Using cell based assays to closely mimic physiological conditions, we observed SNARE-independent translocation of syt9C_2AB to the plasma membrane at calcium levels corresponding to endocrine exocytosis and followed by internalisation to endosomes. The use of point mutants and truncations revealed that initial translocation required only the C_2A domain, whereas the C_2B domain ensured partial pre-binding of syt9C_2AB to the membrane and post-stimulatory localization to endosomes. In contrast to the known properties of neuronal and neuroendocrine syt1 or syt2, the C_2B domain of syt9 did not undergo calcium-dependent membrane binding despite a high degree of structural homology as observed through molecular modelling. These studies demonstrate distinct intracellular properties of syt9 with different roles for each C_2 domain in endocrine cells.

Introduction

Insulin secretion in pancreatic β-cells proceeds by exocytosis of large dense core vesicles and Ca^{2+} constitutes the final trigger for fusion of vesicle and plasma membrane [1, 2]. Synaptotagmins (syt) have been identified as a major Ca^{2+} sensor in neuronal exocytosis based on genetic, electrophysiological and biochemical evidences [3, 4]. They form a family of transmembrane proteins containing two cytosolic C_2 domains, C_2A and C_2B [3, 4]. The most studied synaptotagmins, syt1 and 2, bind phospholipids and SNARE proteins in a Ca^{2+}-dependant fashion via the C_2-domains and thereby attach to lipid membranes and protein complexes involved in exocytosis [3]. In reconstituted systems this mechanism seems to be instrumental for membrane fusion [5]. In addition to their interaction with exocytotic proteins, synaptotagmins may also intervene in endocytosis as suggested in early reports [6]. They are indeed known to interact with several components required for endocytosis [7-9]. Certain observations suggest that this may be mediated by the second C_2-domain, C_2B, although it is probably not its sole function [10-12].

The 16 synaptotagmins currently known can be classified according to their biochemical properties and by sequence alignment [13]. Ca^{2+}-dependant phospholipid binding has been reported for syt1, 2, 3, 5, 7 and 9 [14] and these isoforms have been implicated in the regulation of membrane fusion in different models. In insulin-secreting cells the use of dominant-negatif mutants, recombinant proteins and knock-downs has demonstrated a role in exocytosis for syt1, syt2 and syt9, the latter being the only isoform expressed in primary β-cells [15-17]. Syt9 represents a close homologue to syt1 on sequence alignments with a consensus of 69% (C_2A) and 72% (C_2B), although its structure has not yet been reported. Whereas the kinetics of membrane translocation in the case of syt9 are compatible with endocrine exocytosis, the Ca^{2+}-sensitivity of the cytosolic C_2AB domains is not easily to reconcile [18-20]. In addition, divergent results have been published concerning the ability of the syt9 domains and especially the C_2B domain, to interact with phospholipids and SNARE proteins [21, 22].

In view of the importance of syt9 as an endocrine Ca^{2+} sensor for the exocytosis of large dense core vesicles (LDCVs), we have addressed its translocation and Ca^{2+}-dependency as well as the role of the two C_2 domains herein. We have used cell based assays employing transient expression and fluorescence or biochemical characterisation. This allows also to determine the site of translocation and to circumvent problems inherent to synaptotagmins expressed in bacteria [23, 24]. We now report Ca^{2+}-dependent translocation of C_2AB with an

EC_{50} compatible with endocrine secretion and solely supported by the C_2A domain. In contrast, the C_2B domain impeded translocation but was required for subsequent localization of C_2AB to endocytotic structures.

Materials and methods

Antibodies

The following antibodies were employed: mab anti-T_fR (H 684, Sigma), mab anti-synaptotagmin2, mab anti-synaptotagmin 9 (BD Biosciences, Le-Pont-de-Claix, France), anti-syntaxin (clone HPC1, Sigma, S^t Louis, Missouri, USA), anti-βactin (Abcam, Cambridge, UK), polyclonal anti-eGFP (SantaCruz Biotechnologies, Heidelberg, FRG) and anti-SNAP25 (Sternberger Monoclonals, Covance Research Products, Berkeley, USA); antibodies against chromogranin A, insulin, VAMP2 and synaptophysin were as described [25-27]. HRP-linked anti-mouse or anti-rabbit secondary antibodies were purchased from Amersham Biosciences (Saclay, France); Cy3-labelled anti-mouse secondary antibody was obtained from Jackson ImmunoResearch (Soham, UK).

Plasmids

The plasmid peGFP-Rab7 was kindly provided by B.van Deurs (Panum Institute, Copenhagen, Denmark), peGFP-CD63 by G. Griffiths (Cambridge University, UK), peGFP-Phogrin by W. Almers (Oregon Health Science University, Portland, USA), BONT/C and BOTN/E by H. Niemann, H and T. Binz, (MHH Hannover, FRG) and peGFP-PKC by C. Larsson (University of Lund, Sweden). The vector pRSET-BmStrawberry was generously donated by R. Tsien [28]. The plasmid pKS-Syt2 was as described [15].

Plasmid construction and mutagenesis

cDNA encoding mouse syt9 was generated by RT-PCR from total brain RNA and inserted in a pGEMT-T cloning vector. Truncated syt2 or syt9 was generated by PCR from pGEMT-syt9 or pKS-syt2 plasmids, respectively, using the corresponding sense and antisense primers with an EcoRI site (underligned) inserted in the forward primer and a BamHI in the reverse primer. Primers were as follows: Syt9C_2AB (amino acids 77 to 386), sense primer 5'-TTGGAATTCATGCTGGGCCGGAGTTACATAG-3', antisense primer 5'-TCTGGATCCTCCGGGTGCAGGTATTGGCC-3' ; syt9C_2A (77-233): sense primer 5'-TTGGAATTCATGCTGGGCCGGAGTTACATAG-3', antisense primer 5'-TCTGGATCCAGCCACCTGCAGCTCTCTC-3' ; syt9C_2B (215 - 386): sense primer 5'-TTGGAATTCATGAGTTCAGTGAACCTGG-3', antisense primer: 5'-

TCTGGATCCTCCGGGTGCAGGTATTGGCC-3', syt2C_2AB (101-422): sense primer: 5'-TTGGAATTCATGAAGGGCAAAGGCATGAAG-3', antisense primer: 5'-AGTGGATCCTTGTTCTTGCCCAGAAGAG-3'. The amplified coding sequences were inserted in the EcoRI/BamHI cloning sites either of peGFPN3 (Clontech Laboratories, Palo Alto, CA, USA) for syt9 or in the EcoRI/BamHI cloning sites of peGFPN1 for syt9C_2AB-mStrawberry was constructed by PCR amplification of syt9C_2AB using the primers pairs 5'-CCCAAGCTTATGCTGGGCCGGAGTTACATAG-3';5'-TCTGGATCCGGTCCGGGTGCAGGTATTGGCC-3', HindIII and BamHI sites are underlined. After digestion with HindIII/BamHI, the amplicon was inserted in-frame into pCDNA$_3$-mStrawberry. The pcDNA3-mStrawberry vector was constructed by insertion of the mStrawberry coding sequence into the restriction sites for BamHI and EcoRI of pcDNA3. All constructs were verified by sequencing of both strands. Point mutations were introduced into the syt9 coding sequence leading to the substitution of an aspartic acid (D) to an asparagine (N) using a Quickchange site directed mutagenesis kit (Stratagene, La Jolla, CA, USA) according to the manufacturer's instructions. The forward primers corresponding to each mutation were as follows (exchanged nucleotides given in bold) D145N: 5'-CCTAGGAGGTTCCTCA**A**ATCCCTATGTTAGTGTCT-3'; D197, 199N: 5'-GGTCATGGCGGTGTAT**A**ACTTT**A**ATCGGTTCTCCCGCAACG-3'; D330, 332N: 5'-CTGACTGTTCTG**A**ATTAT**A**ACAAACTGGGGAAGAATGAG-3'.

Cell culture, transient transfection and biochemical membrane translocation assay

MIN6 cells (passage 21 to 30) and HIT-T15 cells (passage 75 to 85) were cultured as described [28, 29]; 72h after plating, MIN6 and HIT-T15 cells were transfected according to the manufacturer's instructions, with plasmids using Lipofectamine™2000 (Invitrogen, Cergy Pontoise, France) or JetPEI™ (PolyPlus-Transfection, Illkirch, France) respectively. HIT-T15 cells seeded at 5x10^4cells/ml 72h prior transfection were grown in 24 well dishes and transfected with plasmid encoding for different cytosolic syt9 fusion proteins. 72 hours after transfection, cells were washed with PBS pH 7.4, detached by PBS-EDTA 10mM and centrifuged at 3000g for 5 minutes at 4°C. Pelleted cells were resuspended and incubated in intracellular buffer (140mM L-glutamic acid/monopotassium salt, 5mM NaCl, 7mM $MgSO_4$, 20 mM HEPES, pH 7, 1µg/ml Aprotinin, 1µg/ml Pepstatin, 1µg/ml Leupeptin, 0.5mM PMSF) either containing 2mM EGTA (non stimulating condition/absence of Ca^{2+}) or 2mM $CaCl_2$ with 10µM ionomycin (stimulating condition/presence of Ca^{2+}) during 5 minutes at 37°

C. Cells were then disrupted by sonication by pulses of 10 second during 1 minute at 4°C [27, 29]. The cell debris and the nuclei were eliminated by a 10 minutes centrifugation at 500g, 4°C. Supernatants were centrifuged at 100 000g during 1 hour 4°C to separate the membrane and the cytosolic fraction. The corresponding samples were suspended in Laemmli buffer, heated at 95°C for 5 minutes and resolved on a 10%SDS-PAGE gel. Proteins were electroblotted onto PVDF, stained, blocked and incubated with the appropriate antibodies [27, 29]. The signal obtained with the chemiluminescence kit ECL Lumi-Light^{Plus} Western Blotting Substrate (Roche Diagnostics, Meylan, France) was detected by a CCD-camera (Roperts Scientific, East Syracuse, NY, USA) and quantified with FluorChem v2.00 (Alpha Innotech Corp., San Leandro, USA) [26].

In vivo membrane translocation assay

MIN6 cells ($1x10^4$ cell/cm^2) grown on 25 mm round glass coverslips were washed twice with 1ml Krebs-Ringer buffer (KRB) pH 7.4 supplemented with 0.05% BSA and 3 mM glucose at 37°C [26, 27]. In experiments using digitonin, cells were incubated in intracellular buffer supplemented with EGTA (0.4mM) and then stimulated in the same buffer with defined Ca^{2+} concentration in presence of 30µM Digitonin. Buffered Ca^{2+} solutions were obtained as described [26, 27] or, in the case of concentrations above 10µM of free Ca^{2+}, calculated using Winmaxc (http://www.stanford.edu/~cpatton/maxc.html) employing the chelators NTA and HEDTA [29]. When ionomycin was used, cells were first incubated in Krebs-Ringer buffer (KRB) pH 7.4 supplemented with 0.05% BSA and 3 mM glucose and stimulation was performed with 1mM Ca^{2+} and 10µM ionomycin in KRB. Cells were kept on a heated microscope stage during acquisition as described [26, 27]. The stimulating buffer were pressure ejected (3 psi, 10s) from a micropipette held at approximately 20µm from the cell. Imaging of living cell was performed at 1 frame/0.5 s using an inverted microscope (Nikon TD300 equipped with a Z-drive) coupled to a monochromator (Till Photonics) and appropriate emission filters. Images were recorded by a CCD-camera (Micromax 1300Y HS, Roperts Scientific) using Metamorph software (Universal Imaging) [30]. The percentage of cells in which translocation was observed was determined as translocation. Due to leakage of unbound syt9-constructs through the pores generated by the detergent, translocation is an all or non event in digitonin-permeabilised cells .

Fluorescence microscopy of fixed cells

MIN6 cells seeded at ($2,6x10^4$cells/cm^2) were grown on 12-mm round glass coverslips and transfected with the corresponding plasmid. 72h after transfection, cells were washed twice with KRB and exposed to either KRB (non stimulating condition) or KRB containing 5mM Ca^{2+} and 10µM ionomycin (stimulating condition) during 10 min at room temperature. Cells were then fixed for 20 minutes at room temperature in 4% paraformaldehyde/PBS in the absence (non stimulating condition) or presence of 5mM $CaCl_2$ (stimulating condition). Coverslips were either directly mounted or stained first with antibodies. In the latter case, coverslips were washed once with KRB and three times with PBS-2% BSA. Permeabilization was performed with 0.1% saponin in PBS-2%BSA for 30 minutes at room temperature and cells were stained with corresponding antibodies. Coverslips were mounted using an antifade kit (VECTASHIELD®Mouting Medium, Vector Laboratories, Burlingame, CA, USA). Imaging was performed on a LMS 510 Meta confocal laser microscope (Zeiss). Colocalization of antibody staining was quantified using Metamorph software (Universal Imaging) by analysing localization and intensities of pixels (n=3) after thresholding. Values are given as mean +/- SEM [28, 30]. Colocalization masks were generated with ImageJ using the plugin "RG2B Colocalization" with a minimum ratio between channels of 0.2 and thresholds of 26 (over 255) for each channel [30].

Molecular modelling

Simulations were carried out for following systems: 1) domain C_2B of synaptotagmin 1 (NM001033680, amino acids 272-421 for modelling) [32] with 12323 water molecules plus 5 Cl^- ions, giving a total of 38.544atoms in an initial box size of 7.37 nm^3. 2) C_2B domain of synaptotagmin 9 (NM016908, amino acids 239-386) with 10967 water molecules plus 12 Cl^- ions giving a total of 34.388 atoms in initial box size of 7.06 nm^3. These systems were solvated with SPC (simple point charge) water and energy minimised. Molecular dynamics simulations were run using Gromacs [33]. A twin-range cut-off was used for longer range interactions: 1nm for Van der Waals interactions and 1.8 for electrostatic interactions. The time step was 2 fs using Shake and NPT conditions were used to constrain bond lengths (i.e., constant number of particles, pressure and temperature in the simulation). A constant pressure of 1 bar was employed in all three directions with a coupling constant of θ_r = 1 ps [34]. Water and protein were coupled separately to a temperature bath at 300 K, with a coupling constant

θ_r = 0.1 ps. The system was equilibrated for 2ns and simulation run for another ns. Results were depicted as ribbon diagrams using VMD 1.8.4 (http://www.ks.uiuc.edu/Research/vmd/).

Statistical analyses

For comparison of two groups, the student's *t*-test was used.

Results

Biochemical characterisation of syt9C_2 domains in situ - In our attempt to investigate the behaviour and translocation of the cytosolic domain of synaptotagmin 9 we have generated constructs and mutants encompassing the C_2A and the C_2B domain (see Fig. 1) and compared it to syt2C_2AB. All constructs harboured a fluorescent protein at their C-terminus, either eGFP or Strawberry [28]. Moreover, point mutations were introduced in the Ca^{2+}-binding sites. Indeed, replacement of cognate aspartates by asparagines in the C_2A domain of synaptotagmin 1 has been shown to abolish partially (D145, numbering for syt9) or completely (D197/199 in syt9) Ca^{2+}-mediated effects of this domain [15, 35]. Similarly, a double mutation in the Ca^{2+}-binding site of the C_2B domain of syt1 (corresponding to D330/D332 of syt9) completely abolishes its function in-vivo [11]. The encoded proteins were expressed in insulin-secreting cells (Fig. 1B) as demonstrated by the use of antibodies against syt9, which also recognized the endogenous forms (left and middle panel), except for syt9C_2B. The protein expressed by this construct did no longer contain the antigenic epitope for the anti-syt9 antibody, but still reacted with anti-eGFP (Fig. 1B, right panel). Note that degradation products of fluorescent proteins were not detected.

We subsequently used these constructs to examine the translocation of syt9 first in a biochemical approach to characterize the behaviour of syt9C_2AB. To this end cells were incubated in the absence or presence of Ca^{2+} (2mM) and ionomycin (10 μM) prior to their fractionation in supernatants (cytosol) and membrane pellets. As shown in Fig. 2A, a considerable amount of syt9C_2AB is already present at membranes in the absence of Ca^{2+} and the cation induces a complete shift of syt9C_2AB to the membrane fraction. Membrane binding of syt9C_2AB is sensitive to a high concentration of salt (Fig. 2B) indicating the electrostatic nature of the interaction. Ca^{2+}-sensitive synaptotagmins bind to the membrane SNARE proteins such as syntaxin or SNAP-25 in a Ca^{2+}-sensitive manner and this interaction is sensitive to the action of clostridial neurotoxins [36-38]. To test whether these SNARE proteins are involved in the translocation observed here, we coexpressed syt9C_2AB and botulinum neurotoxin E or C prior to analysis. Neither of the two toxins altered the Ca^{2+}-sensitive distribution of syt9C_2AB despite cleavage of syntaxin 1 and SNAP25 (Fig. 2C). Note that cleavage was not complete as transient transfection will lead to expression only in a fraction of cells. Taken together these data demonstrate that syt9C_2AB translocates to membranes in response to Ca^{2+} in these insulin-secreting cells. This event occured

independent from SNARE proteins and most likely implies ionic interactions with membrane phospholipids.

We addressed next the role of the different domains of syt9C_2AB in translocation by biochemical means and compared first the C_2 domain of protein kinase C (PKC) with the C_2AB domain of synaptotagmin 2 and 9 (Fig. 3A). Interestingly both, PKC-$C_2\alpha$ and syt2C_2AB, did not bind to membranes in absence of Ca^{2+} in contrast to syt9C_2AB. As expected, a rise in Ca^{2+} resulted in a complete translocation for all three constructs. The first C_2 domain of syt9 alone, syt9C_2A, was largely cytosolic in the absence of Ca^{2+} and fully translocated. It thus behaved as syt2C_2AB and PKC-$C_2\alpha$. Note that a double band was observed as syt9C_2A (arrowhead) migrated just below endogenous syt9 and both were stained by the antibody used. In contrast to the C_2A domain, the C_2B domain remained mainly cytosolic despite the increase in Ca^{2+}. Mutation of D_{145} to asparagine in syt9C_2AB did not alter translocation, whereas mutation of D_{197} and D_{199} rendered syt9C_2AB insensitive to Ca^{2+} (Fig. 3C). We also tested the role of the aspartates in the second C_2 domain known to be required for Ca^{2+} coordination in syt1 and its function in neuroendocytosis [12]. Contrary to the mutations in syt9C_2A, these mutations in the second C_2 domain did not influence the Ca^{2+}-induced distribution of syt9C_2AB. However, syt9C_2AB$_{D330,332N}$ exhibited a considerable increase in membrane binding in the absence of Ca^{2+} similar to the reported observations on the cognate mutation in syt1C_2AB [35].

Modellisation of syt9C_2B domain - To get more insight into the differences between syt1 and syt9 we modelled the structure of syt9C_2B using the published crystal structure of syt1C_2B as a template and performed molecular dynamics simulation after equilibration of the system (Fig. 4). The syt9 sequence showed a striking overall resemblance to syt1 though some differences were apparent. The main distinction concerned the β-sheets 3 and 4 (Fig. 4) which were partially or completely absent in syt9C_2B. Sheet 4 contains seven lysins, which are generally unfavourable for β-sheet formation and modelling has probably failed for this reason to detect the sheets documented previously by NMR and crystallography [31, 37]. As a control, we had modelled syt1C_2B alongside with syt9C_2B and again, both β-sheets partially unfolded or were absent (data not shown). The sole additional, albeit minor difference concerned the C-terminal acidic α-helix H2, which was shorter in syt9C_2B. In contrast, the main Ca^{2+} coordination sites were well conserved and no difference was seen in the spatial

arrangement around β-sheets 6 and 7, from which they emerge. Actually exchange of this portion in syt9C_2B by the corresponding sequence of syt1C_2B conferred "syt1-like" biochemical properties to the mutated syt9C_2B. Thus differences in spatial arrangement do not seem to be responsible for the particular behaviour of syt9C_2B.

Translocation of syt9C_2 domains in living cells - These biochemical assays suggest that the C_2B domain does not positively influence translocation of syt9C_2AB but rather impedes it. However, this approach does not allow determining the nature of the membrane(s) syt9 is binding to and may be influenced by the lengthy fractionation protocol. We therefore resorted to the observation of membrane translocation in living cells by the use of fluorescent videomicroscopy. Moreover, we combined this approach with the use of a detergent, digitonin, to permeabilise the membrane and the use of defined Ca^{2+} buffers to equilibrate intracellular concentrations of the cation [26, 37]. A typical experiment is given in Figure 5A depicting the translocation observed for syt9C_2A and syt9C_2AB. Subsequent to the stimulus and membrane attachment, we observed the disappearance of fluorescent proteins over time. This is most likely due to leakage of fluorescent proteins through the pores formed by digitonin as it was also observed for eGFP itself and only minor bleaching occurred (data not shown). Indeed, chelation of the small volume of calcium ejected from the pipette by EGTA present in the bath solution will rapidly decrease the concentration of free Ca^{2+}. Consequently, even translocated syt9C_2 constructs will detach and dilute in the bath. In the case of syt9C_2B we only observed disappearance of the fluorescence without any attachment to membranes. We also observed some nuclear localization of the fluorescent proteins. This probably represents transiently expressed full-length syt9C_2 constructs, as no degradation products containing eGFP were apparent on immunoblots (see Fig. 1) and the proteins dissolved through the pores arguing against aggregation.

Syt2C_2AB and syt9C_2AB exhibited distinct Ca^{2+} sensitivities EC_{50}s at around 1 μM and 10 μM of free Ca^{2+}, respectively (Fig. 5B). In contrast, syt9C_2A behaved as syt2C_2AB in terms of Ca^{2+} sensitivity in line with our observations in the biochemical assays (see above). Again syt9C_2B remained purely cytosolic and no evidence could be found for translocation (Fig. 5B) and this even on close direct inspection during the experiment or by confocal microscopy (data not shown). This approach also revealed that syt9C_2AB carrying the mutation D_{145}N exhibited some degree of translocation but only at millimolar concentration of free Ca^{2+}, whereas translocation was completely abolished by the double mutation

$D_{197}N/D_{199}N$. Again, the mutation $D_{330}N/D_{332}N$ in the C_2B domain did not alter the Ca^{2+} sensitivity of syt9C_2AB. Thus in both, the biochemical and the in-vivo approaches, the C_2B domain of syt9 actually reduced the Ca^{2+}-sensitivity and the extent of translocation.

Syt9C_2B is required for late translocation to endosomes - On close inspection of films it became apparent that syt9C_2AB rapidly detached from the membrane once the perfusion with buffers containing elevated Ca^{2+} was stopped and translocated to granular intracellular structures. However, as a large amount of syt9C_2AB leaked out of the cell when using digitonin, imaging of those structures was difficult. We therefore used ionomycin and Ca^{2+} as a stimulus to improve visualisation of these structures (Fig. 6A to D). At about 5 s after beginning of membrane translocation staining of these structures became apparent. Most interestingly, the $D_{330}N/D_{332}N$ mutant of syt9C_2AB translocated to the membrane, but never moved subsequently to intracellular structures thus indicating a role for the C_2B domain in the second step. Syt9C_2B alone never translocated and both mutants of the C_2A Ca^{2+}–binding site (syt9C_2AB $D_{145}N$ and $D_{197,199}N$) failed to translocate to the plasma membrane under the conditions used here (intact cells, ionomycin) and were not found on intracellular structures (data not shown). It seems therefore that prior passage to the plasma membrane is required for localization on the intracellular structures.

In view of the requirement of the C_2B domain for this event we attempted to characterize the compartment(s) involved by coexpression of fluorescent fusion proteins and the use of antibodies. As the fusion proteins used as marker were tagged with eGFP, we used syt9C_2AB linked to the fluorescent protein Strawberry (syt9C_2AB-S) known to be monomeric [28]. Syt9C_2AB-S behaved as syt9C_2AB-eGFP and colocalized with eGFP tagged syt9 upon cotransfection (data not shown). To exclude a potential interaction between fluorescent proteins, we tested the combination of syt9C2AB-S and LPH-eGFP, a plasma membrane marker [29, 30] and SVP38-eGFP [39]. Neither of these constructs colocalized with syt9C_2AB-S suggesting that interactions between fluorescent proteins did not play any significant role (data not shown). A considerable number of compartments tested using antibodies did also not reveal any substantial degree of colocalisation such as SNAP-25, syntaxin 1, VAMP2/synaptobrevin2, insulin and chromogranin A. This excluded compartments harbouring these SNARE proteins or secretory granules as localizationlocalization for syt9C_2AB-eGFP. In contrast, we observed a high degree of colocalization for the endosomal markers CD63-eGFP [40] and rab7-eGFP [41] in fixed cells

(see Fig. 7A and C). In addition, colocalization was evident for phogrin-eGFP, known to be recycled through endosomal pathways [42], and to a lesser degree for the transferrin receptor (TfR). We also determined whether colocalization can be observed in living cells by videomicroscopy (see Fig. 7 B). Indeed, a considerable degree of colocalization was apparent for Rab7-eGFP and syt9C_2AB-S after stimulation of cells with ionomycin. These observations are in line with an attachment of syt9C_2AB to endosomal membranes.

Biochemical Journal Immediate Publication. Published on 29 Jan 2007 as manuscript BJ20061182

Discussion

Synaptotagmins play a major role as Ca^{2+} sensor in exocytotic membrane fusion and in endocytosis [43, 44]. Despite a considerable conservation in the Ca^{2+} and phospholipid-binding C_2 domains among several isoforms, such as syt1, 2 and 9, differences are apparent which may be of functional importance. Our data indicate that the C_2AB domain of synaptotagmin 9 is operational in living cells at Ca^{2+} levels present during exocytosis in pancreatic β-cells [20, 45]. In contrast to syt1, however, the C_2B domain lowers the Ca^{2+}-affinity for membrane translocation, but is required for ensuing localization on endosomal structures.

In contrast to previous studies, we used transient expression of synaptotagmins in mammalian cells for our biochemical and fluorescent assays. Although liposomal systems permit a good control of the variables, they do not reproduce the lipid composition or membrane protein/lipid ratio present in native preparations as glycerophospholipids are largely overrepresented. It is thus important to obtain affinities at intracellular conditions. Moreover, the use of recombinant synaptotagmins expressed in bacteria has been difficult due to precipitation [46, 47] or to the presence of contaminants [23, 24]. Our initial biochemical characterization revealed that the interactions are sensitive to ionic forces and can occur independently from SNARE proteins. Indeed, their cleavage by clostridial neurotoxins did not alter the distribution or extent of translocation. Note that divergent results on Ca^{2+}-dependant binding of syt9C_2AB to SNARE proteins had been reported [18, 21]. Our observation does not exclude a role for the interaction with SNARE proteins in the membrane attachment of syt9, as they may direct synaptotagmins to specific sites, or in the function of syt9 during membrane fusion, which was not tested here.

Two major differences were apparent here when comparing the C_2AB domains of syt9 and syt2. First, in both assays syt9C_2AB was already in part attached to the membrane in non-stimulated living cells or in the absence free Ca^{2+} in biochemical assays, whereas syt2C_2AB was completely cytosolic under those conditions. The differential membrane attachment of the two isoforms in the absence of Ca^{2+} has been observed in some but not all liposome-based assays using phosphatidylcholine/phosphatidylserine vesicles and was more pronounced in the presence of PIP_2 [21, 22]. Cleavage of SNARE proteins by clostridial neurotoxins did not diminish the attachment in the absence of Ca^{2+} in our assays. Interestingly, neither syt9C_2A alone nor syt9C_2B alone demonstrated any membrane binding in the absence of Ca^{2+}. Pre-binding of syt9C_2AB to membranes is therefore independent of SNARE proteins and requires cooperation between the two C_2 domains. Second, the EC_{50} for

Ca^{2+} required in membrane translocation differed by one order of magnitude between syt2C_2AB and syt9C_2AB. Interestingly, syt9C_2A alone was indistinguishable from syt2C_2AB in this term. The most likely explanation is provided by the increased pre-binding of syt9 in presence of the C_2B domain which abolishes a high affinity component. Importantly, the EC_{50} observed here for syt9C_2AB in living cells corresponds well with the values reported for Ca^{2+} evoked exocytosis of insulin [20, 45].

Whereas the C_2A domains of syt9 behaved as expected, the C_2B domain clearly differed from syt2C_2B in respect to reported Ca^{2+}-dependent membrane binding [22, 48]. As to the behaviour of the C_2B domain, divergent results have been reported using either the C_2B domain only [21] or a C_2B domain containing in addition 23 amino acids of the sequence linking C_2A and C_2B [22]. Our modelling data support the notion that amino acids 238 to 386 are sufficient to form a stable C_2B domain and additional N-terminal residues are not required. The observations reported here clearly indicate that syt9C_2B is not capable to translocate in the cellular environment. This difference is surprising in view of the high degree of sequence conservation as well as structural arrangement between the isoforms. As membrane attachment of syt1C_2B is less resistant to salt washes than syt1C_2A, minor changes in the C_2B domain may be important [49]. Indeed, domain swapping between syt1 and syt9 around loop 3 restored Ca^{2+} sensitivity [21]. As the structure of this sequence part is conserved between the two isoforms in modelling, very subtle changes may be responsible for their distinct behaviour.

Although syt9C_2B was fully dispensable for Ca^{2+}-dependent membrane translocation, it was clearly implicated in the subsequent attachment to intracellular structures as syt9C_2AB$_{D330,332N}$ still translocated to the plasma membrane, but was not internalised. Although syt9C_2B does not bind Ca^{2+} in accordance to indirect assays as performed here and by others [21], the mutation C_2AB$_{D330,332N}$ is located at the base of a loop directed towards the membrane and may thus destabilise interactions [50]. Intracellular targeting of syt1C_2A has been reported but was mainly directed to the trans-Golgi network in MDCK kidney cells in contrast to our observation on both C_2 domains of syt9 [51]. The reported localization may reflect distinct affinities for certain phosphoinositols or SNARE proteins. The codistribution of marker proteins observed here for syt9C_2AB is compatible with late endosomes as a major location and a minor location on early endosomes. Syt9 has been reported previously on endocytotic compartments in mast cells and syt9C_2B interacts with the clathrin adaptor complex AP-2, as had been shown for other synaptotagmins [7, 52]. This provides a potential mechanism for internalisation. As targeting to the intracellular structures required the

presence of the C_2A domain, we reckon that prior contact with the plasma membrane is required. Probably the fluorescent protein accompanies membrane internalisation, but is not directly transferred from the cytosol to endosomes. The functional implication is yet unclear in the case of syt9. The C_2B domain of syt1 is implicated in the regulation of endocytosis and interestingly requires the Ca^{2+}-coordinating aspartates in C_2B cognate to those which abolished internalisation of syt9C_2AB [53].

What might be the functional outcome of the differences between syt1 and syt9 in terms of C_2 domains? Whereas in clonal β-cells syt1, 2 and 9 are expressed on LDCVs and function in exocytosis, primary cells contain seemingly only syt9 and this isoform should therefore not be a redundant Ca^{2+}-sensor [15-17, 54]. The Ca^{2+} dependency of syt9C_2AB fits well with the physiological Ca^{2+} requirements for insulin exocytosis and the observed right shift may be compensated by pre-binding to the membrane via the C_2B domain. Such a mechanism may be an advantage in a cell that secretes mainly at limited time periods, i.e. in response to nutritional stimuli.

References

1 Henquin, J. C. (2004) Pathways in beta-cell stimulus-secretion coupling as targets for therapeutic insulin secretagogues. Diabetes **53 Suppl. 3**, S48-58

2 Lang, J. (1999) Molecular mechanisms and regulation of insulin exocytosis as a paradigm of endocrine secretion. Eur. J. Biochem. **259**, 3-17

3 Jahn, R., Lang, T. and Sudhof, T. C. (2003) Membrane fusion. Cell **112**, 519-533

4 Sudhof, T. C. (2004) The synaptic vesicle cycle. Annu. Rev. Neurosci. **27**, 509-547

5 Bhalla, A., Chicka, M. C., Tucker, W. C. and Chapman, E. R. (2006) Ca^{2+}-synaptotagmin directly regulates t-SNARE function during reconstituted membrane fusion. Nat. Struct. Mol. Biol. **13**, 323-330

6 DiAntonio, A., Parfitt, K. D. and Schwarz, T. L. (1993) Synaptic transmission persists in synaptotagmin mutants of Drosophila. Cell **73**, 1281-1290

7 Zhang, J. Z., Davletov, B. A., Sudhof, T. C. and Anderson, R. G. (1994) Synaptotagmin I is a high affinity receptor for clathrin AP-2: implications for membrane recycling. Cell **78**, 751-760

8 von Poser, C., Zhang, J. Z., Mineo, C., Ding, W., Ying, Y., Sudhof, T. C. and Anderson, R. G. (2000) Synaptotagmin regulation of coated pit assembly. J. Biol. Chem. **275**, 30916-30924

9 Fergestad, T. and Broadie, K. (2001) Interaction of Stoned and Synaptotagmin in Synaptic Vesicle Endocytosis. J. Neurosci. **21**, 1218-1227

10 Llinas, R. R., Sugimori, M., Moran, K. A., Moreira, J. E. and Fukuda, M. (2004) Vesicular reuptake inhibition by a synaptotagmin I C2B domain antibody at the squid giant synapse. Proc. Nat'l Acad. Sci. U S A **101**, 17855-17860

11 Mackler, J. M., Drummond, J. A., Loewen, C. A., Robinson, I. M. and Reist, N. E. (2002) The C_2B Ca^{2+}-binding motif of synaptotagmin is required for synaptic transmission in vivo. Nature **418**, 340-344

12 Earles, C. A., Bai, J., Wang, P. and Chapman, E. R. (2001) The tandem C_2 domains of synaptotagmin contain redundant Ca^{2+} binding sites that cooperate to engage t-SNAREs and trigger exocytosis. J. Cell Biol. **154**, 1117-1124

13 Craxton, M. (2004) Synaptotagmin gene content of the sequenced genomes. BMC Genomics **5**, 43

14 Rickman, C., Craxton, M., Osborne, S. and Davletov, B. (2004) Comparative analysis of tandem C2 domains from the mammalian synaptotagmin family. Biochem. J. **378**, 681-686

15 Lang, J., Fukuda, M., Zhang, H., Mikoshiba, K. and Wollheim, C. B. (1997) The first C2 domain of synaptotagmin is required for exocytosis of insulin from pancreatic β-cells: action of synaptotagmin at low micromolar calcium. EMBO J. **16**, 5837-5846

16 Gut, A., Kiraly, C. E., Fukuda, M., Mikoshiba, K., Wollheim, C. B. and Lang, J. (2001) Expression and localization of synaptotagmin isoforms in endocrine β-cells: their function in insulin exocytosis. J. Cell Sci. **114**, 1709-1716

17 Iezzi, M., Eliasson, L., Fukuda, M. and Wollheim, C. B. (2005) Adenovirus-mediated silencing of synaptotagmin 9 inhibits Ca^{2+}-dependent insulin secretion in islets. FEBS Lett. **579**, 5241-5246

18 Bhalla, A., Tucker, W. C. and Chapman, E. R. (2005) Synaptotagmin isoforms couple distinct ranges of Ca^{2+}, Ba^{2+}, and Sr^{2+} concentration to SNARE-mediated membrane fusion. Mol. Biol. Cell **16**, 4755-4764

19 Rorsman, P., Eliasson, L., Renstrom, E., Gromada, J., Barg, S. and Gopel, S. (2000) The cell physiology of biphasic insulin secretion. News Physiol. Sci. **15**, 72-77

20 Vallar, L., Biden, T. J. and Wollheim, C. B. (1987) Guanine nucleotides induce Ca^{2+}-independent insulin secretion from permeabilized RINm5F cells. J. Biol. Chem. **262**, 5049-5056

21 Shin, O. H., Maximov, A., Lim, B. K., Rizo, J. and Sudhof, T. C. (2004) Unexpected Ca^{2+}-binding properties of synaptotagmin 9. Proc. Nat'l Acad. Sci. U S A **101**, 2554-2559

22 Tucker, W. C., Edwardson, J. M., Bai, J., Kim, H. J., Martin, T. F. and Chapman, E. R. (2003) Identification of synaptotagmin effectors via acute inhibition of secretion from cracked PC12 cells. J. Cell Biol. **162**, 199-209

23 Shin, O. H., Rhee, J. S., Tang, J., Sugita, S., Rosenmund, C. and Sudhof, T. C. (2003) Sr^{2+} binding to the Ca^{2+} binding site of the synaptotagmin 1 C_2B domain triggers fast exocytosis without stimulating SNARE interactions. Neuron **37**, 99-108

24 Ubach, J., Lao, Y., Fernandez, I., Arac, D., Sudhof, T. C. and Rizo, J. (2001) The C2B domain of synaptotagmin I is a Ca^{2+}-binding module. Biochemistry **40**, 5854-5860

25 Boal, F., Le Pevelen, S., Ciepluch, C., Scotti, P. and Lang, J. (2006) Cysteine-string protein isoform β (Cspβ) is targeted to the trans-Golgi network as a non-palmitoylated CSP in clonal β-cells. Biochim. Biophys. Acta – Mol. Cell Res. [Epub ahead of print]

26 Boal, F., Zhang, H., Tessier, C., Scotti, P. and Lang, J. (2004) The variable C-terminus of cysteine string proteins modulates exocytosis and protein-protein interactions. Biochemistry **43**, 16212-16223

27 Monterrat, C., Boal, F., Grise, F., Hemar, A. and Lang, J. (2006) Synaptotagmin 8 is expressed both as a calcium-insensitive soluble and membrane protein in neurons, neuroendocrine and endocrine cells. Biochim. Biophys. Acta – Mol. Cell Res. **1763**, 73-81

28 Shaner, N. C., Steinbach, P. A. and Tsien, R. Y. (2005). A guide to choosing fluorescent proteins. Nat. Methods **2**, 905-909.

29 Lajus, S., Vacher, P., Huber, D., Dubois, M., Benassy, M. N., Ushkaryov, Y. and Lang, J. (2006) α-latrotoxin induces exocytosis by inhibition of voltage-dependent K^+ channels and by stimulation of L-type Ca^{2+} channels via latrophilin in β-cells. J. Biol. Chem. **281**, 5522-5531

30 Lajus, S. and Lang, J. (2006) Splice variant 3, but not 2 of receptor protein-tyrosine phosphatase σ can mediate stimulation of insulin-secretion by α-latrotoxin. J. Cell. Biochem. **98,** 1552-1559

31 Rasband, W. S. ImageJ. U. S. National Institutes of Health, Bethesda, Maryland, USA, http://rsb.info.nih.gov/ij/ 1997-2006

32 Cheng, Y., Sequeira, S. M., Malinina, L., Tereshko, V., Sollner, T. H. and Patel, D. J. (2004) Crystallographic identification of Ca^{2+} and Sr^{2+} coordination sites in synaptotagmin I C_2B domain. Protein Sci. **13**, 2665-2672

33 van Aalten, D. M., Amadei, A., Linssen, A. B., Eijsink, V. G., Vriend, G. and Berendsen, H. J. (1995) The essential dynamics of thermolysin: confirmation of the hinge-bending motion and comparison of simulations in vacuum and water. Proteins **22**, 45-54

34 Berendsen, H. J. C., Postma, J. P. M., van Gunsteren, W. F., DiNola, A. and Haak, J. R. (1984) Molecular dynamics with coupling to an external bath. J. Chem. Phys. **81**, 3684-3690

35 Robinson, I. M., Ranjan, R. and Schwarz, T. L. (2002) Synaptotagmins I and IV promote transmitter release independently of Ca^{2+} binding in the C_2A domain. Nature **418**, 336-“40

36 Jahn, R. and Niemann, H. (1994) Molecular mechanisms of clostridial neurotoxins. Ann. N. Y. Acad. Sci. **733**, 245-é55

37 Lang, J., Regazzi, R. and Wollheim, C. B. (1997) in Bacterial toxins: tools in cell biology (Aktories, K., ed.), pp. 217-240, Chapman & Hall, Weinheim

38 Lang, J., Zhang, H., Vaidyanathan, V. V., Sadoul, K., Niemann, H. and Wollheim, C. B. (1997) Transient expression of botulinum neurotoxin C1 light chain differentially inhibits calcium and glucose induced insulin secretion in clonal β-cells. FEBS Lett **419**, 13-17

39 Kaether, C., Skehel, P. and Dotti, C. G. (2000) Axonal membrane proteins are transported in distinct carriers: a two-color video microscopy study in cultured hippocampal neurons. Mol. Biol. Cell **11**, 1213-1224

40 Kobayashi, T., Vischer, U. M., Rosnoblet, C., Lebrand, C., Lindsay, M., Parton, R. G., Kruithof, E. K. and Gruenberg, J. (2000) The tetraspanin CD63/lamp3 cycles between endocytic and secretory compartments in human endothelial cells. Mol. Biol. Cell **11**, 1829-&_43

41 Vonderheit, A. and Helenius, A. (2005) Rab7 Associates with Early Endosomes to Mediate Sorting and Transport of Semliki Forest Virus to Late Endosomes. PLoS Biology **3,** e233 doi:10.1371/journal.pbio.0030233

42 Vo, Y. P., Hutton, J. C. and Angleson, J. K. (2004) Recycling of the dense-core vesicle membrane protein phogrin in Min6 β-cells. Biochem. Biophys. Res. Commun. **324**, 1004-1010

43 Geppert, M., Goda, Y., Hammer, R. E., Li, C., Rosahl, T. W., Stevens, C. F. and Sudhof, T. C. (1994) Synaptotagmin I: a major Ca^{2+} sensor for transmitter release at a central synapse. Cell **79**, 717-727

44 Nicholson-Tomishima, K. and Ryan, T. A. (2004) Kinetic efficiency of endocytosis at mammalian CNS synapses requires synaptotagmin I. Proc. Nat'l Acad. Sci. U S A **101**, 16648-16652

45 Bokvist, K., Eliasson, L., Ammala, C., Renstrom, E. and Rorsman, P. (1995) Co-localization of L-type Ca^{2+} channels and insulin-containing secretory granules and its significance for the initiation of exocytosis in mouse pancreatic B-cells. EMBO J. **14**, 50-57

46 Damer, C. K. and Creutz, C. E. (1996) Calcium-dependent self-association of synaptotagmin I. J. Neurochem. **67**, 1661-1668

47 Elferink, L. A., Peterson, M. R. and Scheller, R. H. (1993) A role for synaptotagmin (p65) in regulated exocytosis. Cell **72**, 153-159

48 Li, C., Ullrich, B., Zhang, J. Z., Anderson, R. G., Brose, N. and Sudhof, T. C. (1995) Ca^{2+}-dependent and -independent activities of neural and non-neural synaptotagmins. Nature **375**, 594-599

49 Hui, E., Bai, J. and Chapman, E. R. (2006) Ca^{2+}-triggered simultaneous membrane penetration of the tandem C_2-domains of synaptotagmin I. Biophys. J. **91**, 1767-1777

50 Rufener, E., Frazier, A. A., Wieser, C. M., Hinderliter, A. and Cafiso, D. S. (2005) Membrane-bound orientation and position of the synaptotagmin C2B domain determined by site-directed spin labeling. Biochemistry **44**, 18-28

51 Evans, J. H., Gerber, S. H., Murray, D. and Leslie, C. C. (2004) The calcium binding loops of the cytosolic phospholipase A2 C2 domain specify targeting to Golgi and ER in live cells. Mol. Biol. Cell **15**, 371-383

52 Haberman, Y., Ziv, I., Gorzalczany, Y., Fukuda, M. and Sagi-Eisenberg, R. (2005) Classical protein kinase C(s) regulates targeting of synaptotagmin IX to the endocytic recycling compartment. J. Cell Sci. **118**, 1641-1649

53 Poskanzer, K. E., Fetter, R. D. and Davis, G. W. (2006) Discrete residues in the C_2B domain of synaptotagmin I independently specify endocytic rate and synaptic vesicle size. Neuron **50**, 49-62

54 Xiong, X., Zhou, K. M., Wu, Z. X. and Xu, T. (2006) Silence of synaptotagmin I in INS-1 cells inhibits fast exocytosis and fast endocytosis. Biochem. Biophys. Res. Commun. **347**, 76-82

Figure Legends

Fig. 1. Expression of synaptotagmin 2 and synaptotagmin 9 constructs. (A) Schematic diagram representing the different syt9 and syt2 constructs used: syt2C_2AB (101-422), syt9C_2AB (77-386), syt9C_2A (77-233) and syt9C_2B (215-386). Mutation of aspartate to asparagin in the C_2A and/or the C_2B domains gave rise to $D_{145}N$, $D_{197}N$, $D_{199}N$, $D_{330}N$, $D_{332}N$. All constructs are C-terminally tagged with a fluorescent protein (FP). (B) Expression of the constructs in HIT T15 cells. Cells were transfected with the different variants. 72h after transfection, cells were harvested and 20µg of total proteins were separated by SDS-PAGE and immunoblotted with anti-syt2, anti-syt9 (BD) or anti-eGFP antibodies. The lane number corresponds to the construct number.

Fig. 2. Membrane binding of syt9C_2AB-eGFP in HIT-T15 cells. (A) 72h after transfection with syt9C_2AB-eGFP, HIT-T15 cells were incubated 5 min at 37°C in presence of Ca^{2+} (2mM $CaCl_2$ supplemented with 10µM ionomycin) or in absence of Ca^{2+} (2mM EGTA) and fractioned by ultracentrifugation at 100.000g. Distribution of syt9C_2AB-eGFP in supernatants (c) and membrane pellets (m) were analysed by western blot using antibodies against syt9 and against the transmembrane protein syntaxin 1 as a control for fractionation. The distribution was quantified by densitometry as given by the histogram (on the right), S.D.s are indicated (n=8). (B) Transfected cells are incubated in absence or in presence of Ca^{2+} supplemented with 0.5M KCl. Fractionation and analysis was performed as above, n=3. (C) HIT-T15 cells were co-transfected with syt9C_2AB-eGFP and plasmids coding for botulinum neurotoxins BoNT/C and BoNT/E. Translocation and the effect of each toxin were analysed by immunoblotting using anti-syt9, anti-syntaxin1 or anti-SNAP25 antibodies. Errors bars represent the S.D. (n=3); *, $2p<0.05$ as compared to membranes.

Fig. 3. The C_2A but not the C_2B domain is responsible of Ca^{2+}-dependant binding of syt9 to membranes. (A) HIT-T15 cells expressing PKC-$C_2\alpha$-eGFP , syt2C_2AB-eGFP and syt9C_2AB-eGFP were incubated 5min at 37°C in presence (2mM $CaCl_2$, 10µM ionomycin) or absence of Ca^{2+} (2mM EGTA). The subsequent fractionation was analysed by western blot using anti-GFP, anti-syt2 or anti-syt9 antibodies for PKC-$C_2\alpha$-eGFP, syt2C_2AB-eGFP and syt9C_2AB-eGFP, respectively. Histograms on the right represent the distribution of the protein quantified

by densitometry. Errors bars represent the S.D (n=3); *, 2p<0.05 as compared to membranes. (B) The same experiments in (A) were performed on HIT-T15 cells transfected with syt9C_2A-eGFP and syt9C_2B-eGFP. Syt9C_2A-eGFP, was revealed with the anti-syt9 antibody that detected the fluorescent protein (indicated by arrowhead) and the endogenous protein. Syt9C_2B-eGFP was revealed with the anti-GFP antibody as it does not contain the epitope for the anti-syt9 antibody. (C) Syt9C_2AB-eGFP and its mutants were detected using anti-syt9.

Fig. 4. Molecular simulation of syt9C_2B domain. Ribbon diagrams are shown. A: syt1C_2B according to crystal structure 1UOW. B: C_2B domain of syt9 after 3 ns simulation. The loops 1 and 3 (L1, L3), the mutation $D_{330}N/D_{332}N$ (asterisks), the unstructured part corresponding to the β-sheet 4 in syt1 and the shortened α-helix H2 are indicated. Views are given to highlighten differences between the structures.

Fig. 5. Stimulation of living cells by low micromolar Ca^{2+} translocates the C_2A, but not the C_2B domain of syt9. (A) MIN6 cells expressing syt9C_2AB-eGFP, syt9C_2A-eGFP or syt9C_2B-eGFP were grown on coverslip and stimulated by pressure ejection of buffer containing 10µM of free Ca^{2+} supplemented with 30µM digitonin**.** Cells were imaged at 37° C by time-lapse microscopy. Images **a, c** and **e** were taken 0 sec and, **b**,**d** and **f** 3 sec after stimulation. (B) Membrane binding affinity of syt9 variants. Experiments are performed in MIN6 cells as described in A. Defined concentrations of free Ca^{2+} supplemented with digitonin were used to stimulate the cells.

Fig. 6. Syt9C_2AB–eGFP but not syt9$C_2AB_{D330/332N}$–eGFP distributes to intracellular structures after stimulation with Ca^{2+}. MIN6 cells expressing syt9C_2AB-eGFP (A, B, C) or syt9$C_2AB_{D330/332N}$-eGFP (E, F, G) were stimulated by 5mM $CaCl_2$ and 10µM ionomycin. The distribution of the two fusion proteins was imaged and the three panels represent the distribution of the proteins at 0 sec (A, E), 10 sec (B, F) and 20 sec after stimulation (C, G). GFP fluorescence was quantified in 2 different areas corresponding to plasma membrane (Zone 1) and to the intracellular space (Zone 2) (D, H). F_o: fluorescence at t = 0 sec F_t: fluorescence at t. Images are representative of at least ten independent experiments.

Fig. 7. Syt9C_2AB redistributes to endosomes. MIN6 cells transfected with indicated constructs were incubated for 10 min at room temperature in the presence of Ca^{2+} (5mM $CaCl_2$, ionomycin 10μM) to allow the translocation of syt9C_2AB-FP (eGFP or S, strawberry) to the plasma membrane and to intracellular structure. Images corresponding to the different channels are given in the left and middle column, colocalization as indicated by MERGE in the right column. TfR, transferring receptor; EEA1, early endosomal antigen. A: cells were subsequently fixed and colocalization of the FP constructs analysed by confocal microscopy. B: living cells observed by videomicroscopy 10 min after stimulation. C: Percentage of colocalization given as obtained from at least five experiments.

FIG. 1

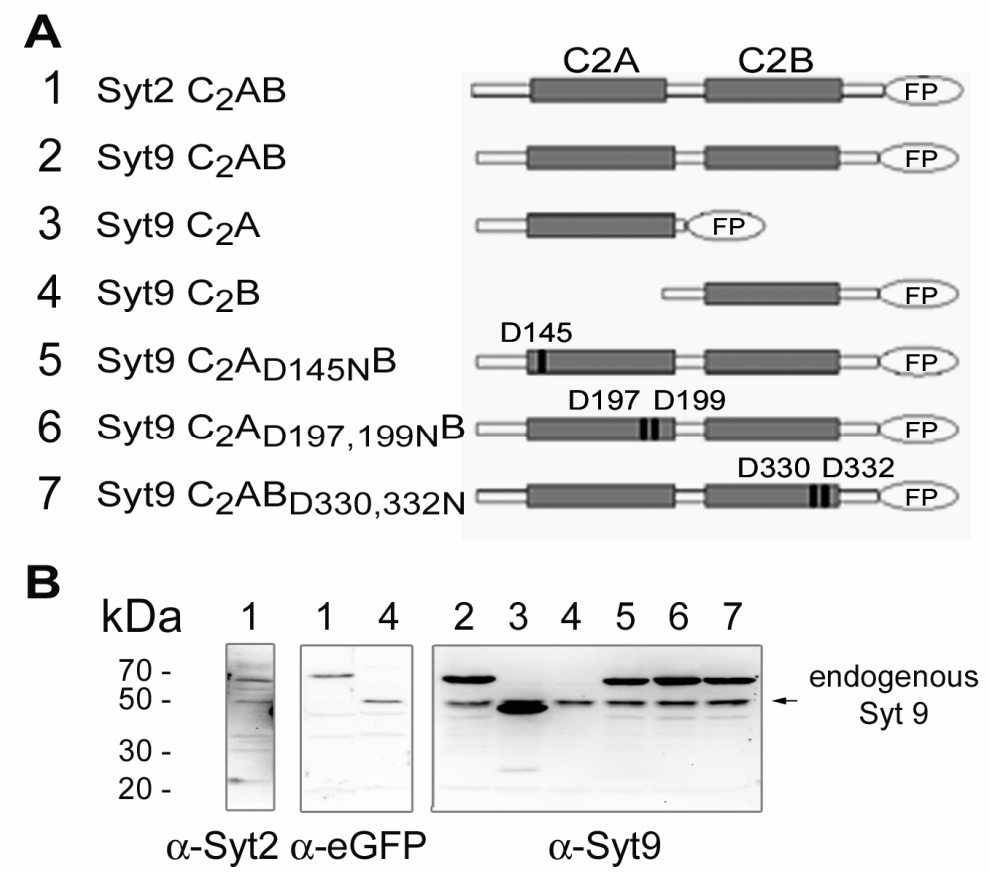

FIG. 2

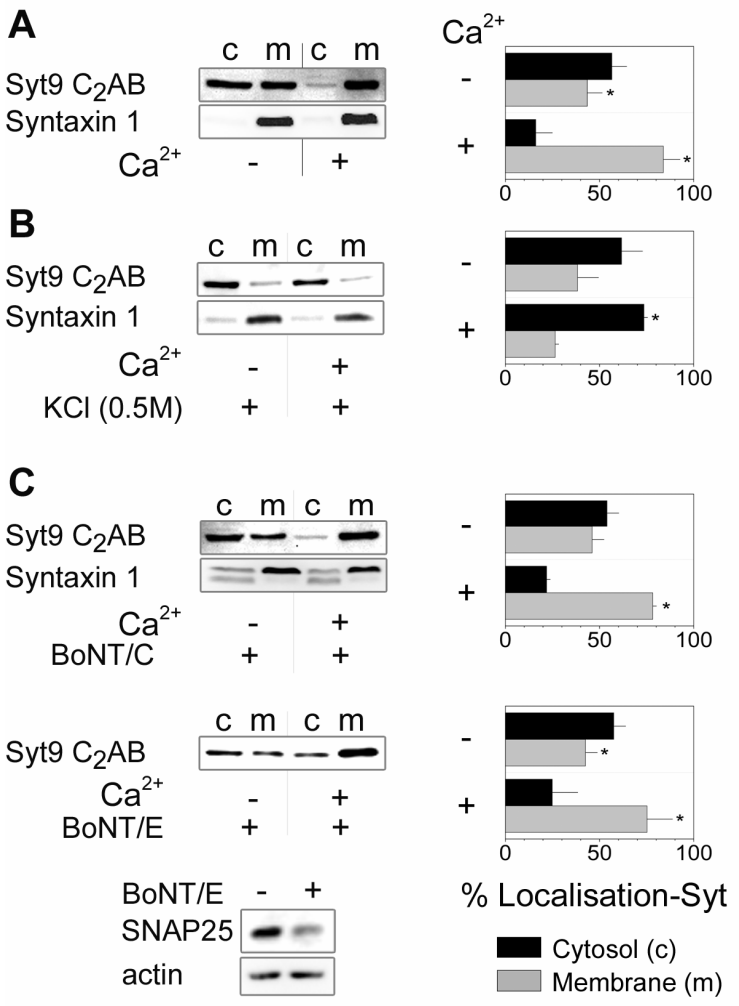

Biochemical Journal Immediate Publication. Published on 29 Jan 2007 as manuscript BJ20061182

FIG. 3

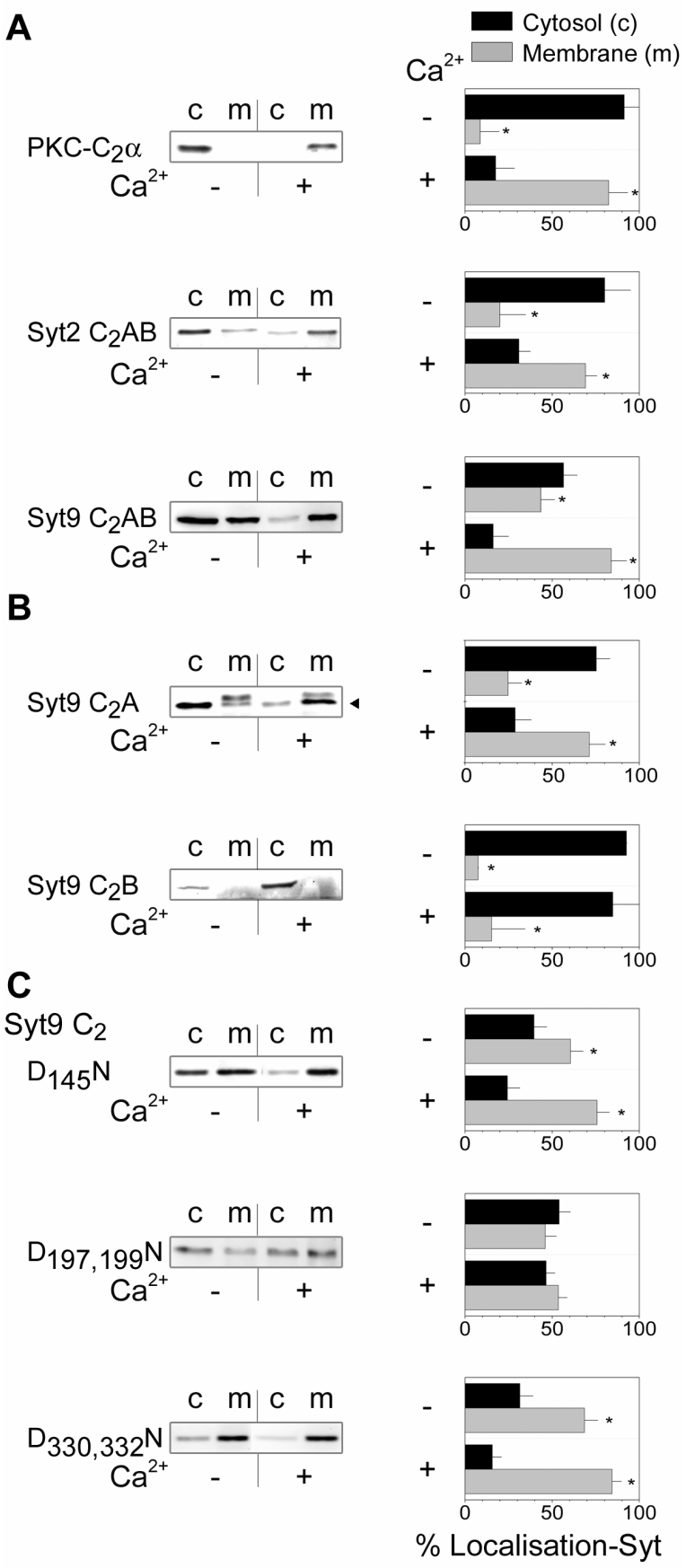

Biochemical Journal Immediate Publication. Published on 29 Jan 2007 as manuscript BJ20061182

FIG. 4

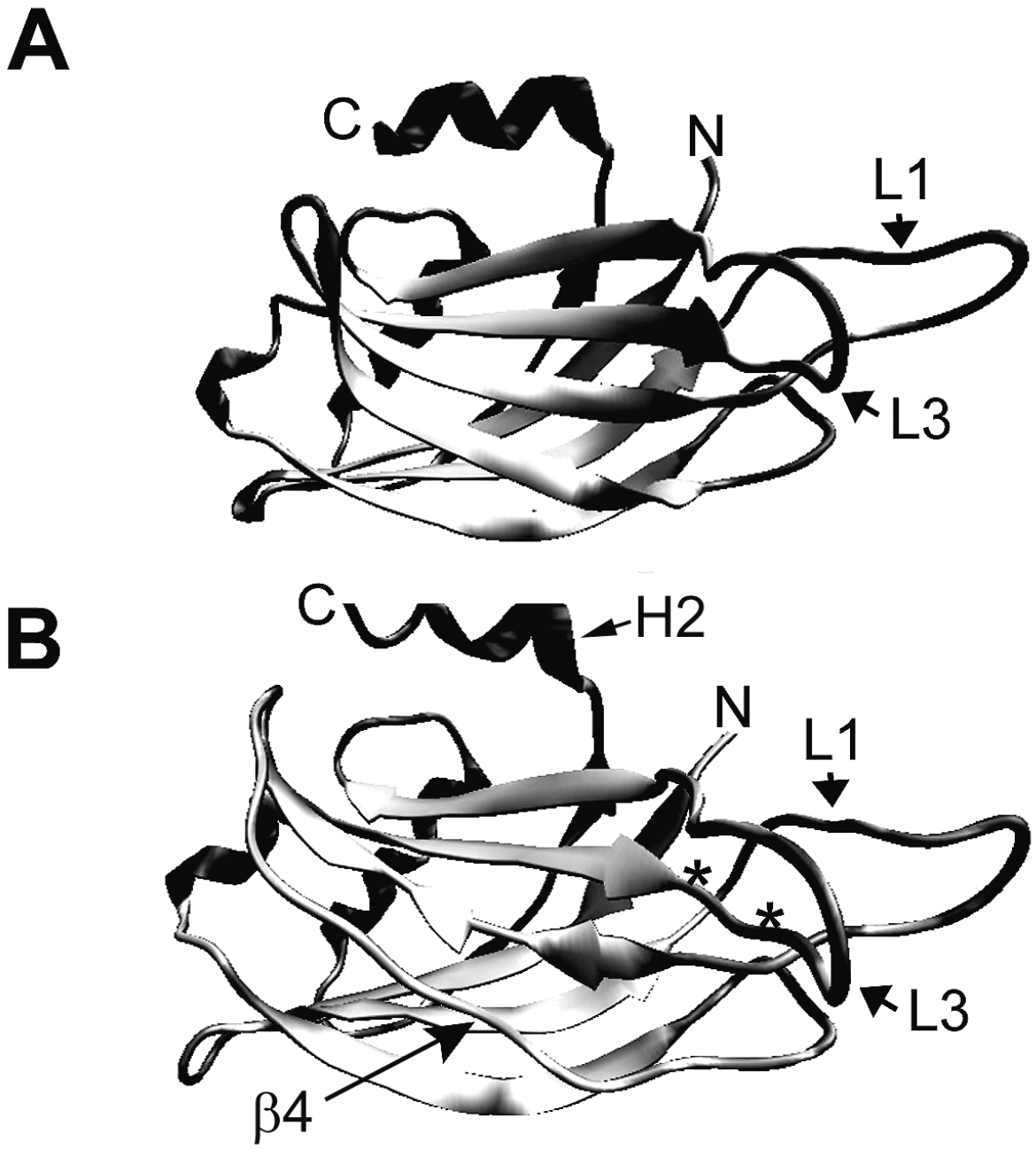

FIG. 5

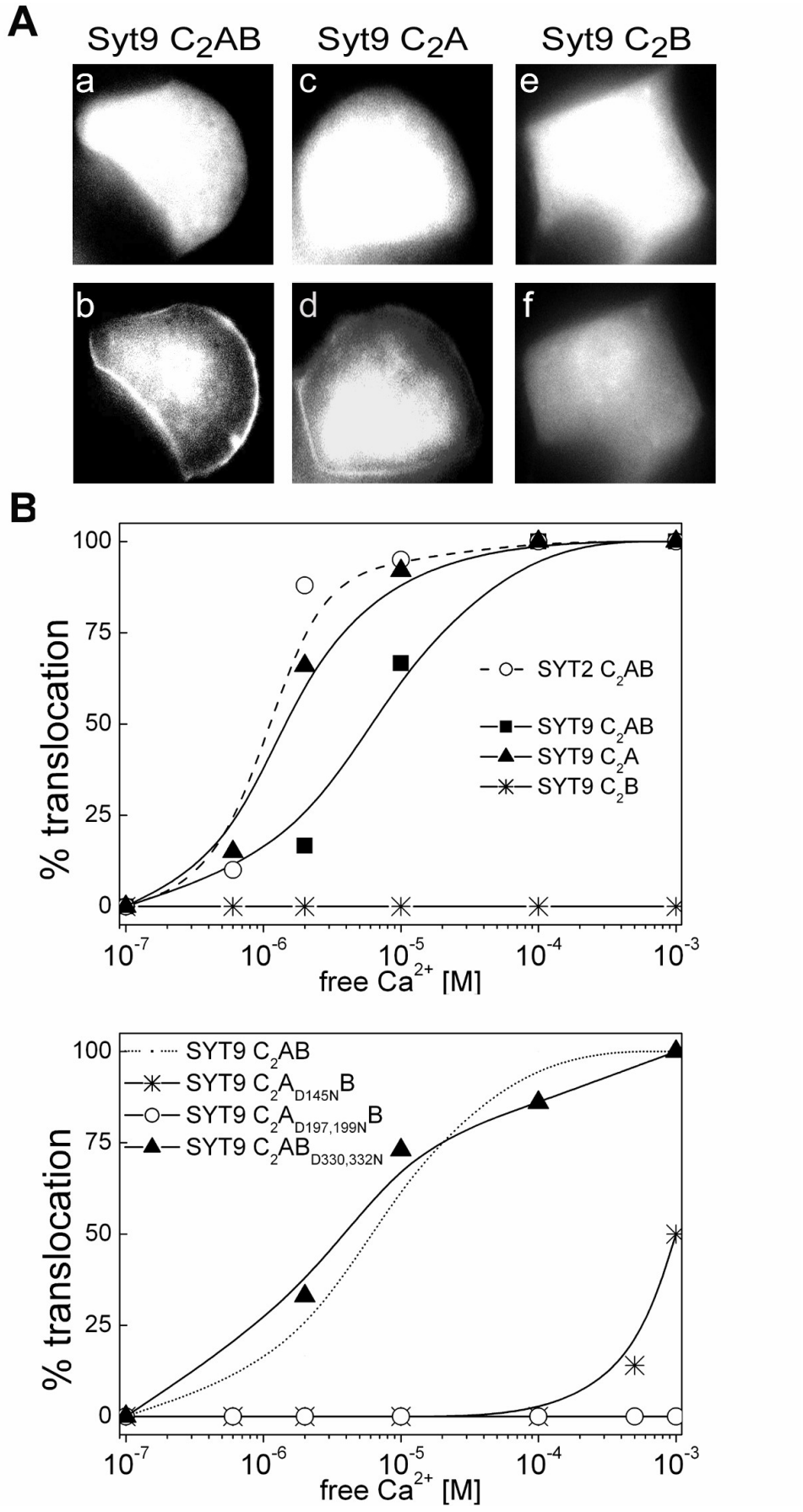

FIG. 6

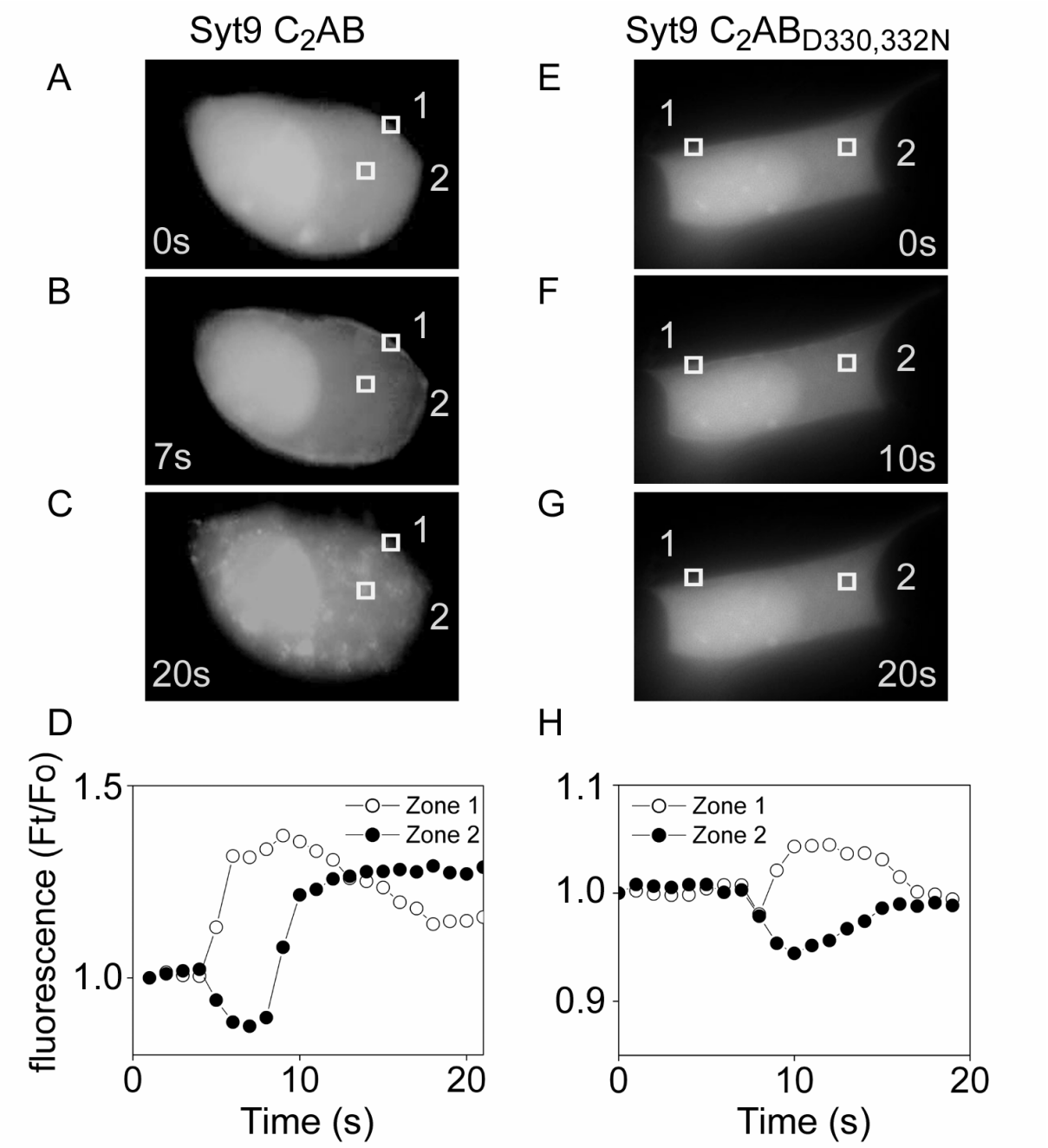

FIG. 7